Evolution of the multiband RKKY interaction: Application to iron pnictides and chalcogenides

Alireza Akbari[1], **Peter Thalmeier**[1], **and Ilya Eremin**[2]

[1] Max-Planck Institute for the Chemical Physics of Solids, D-01187 Dresden, Germany

[2] Theoretische Physik III, Ruhr-Universität Bochum, D-44780, Bochum, Germany

E-mail: akbari@cpfs.mpg.de

Abstract. The indirect RKKY interaction in iron pnictide and chalcogenide metals is calculated for a simplified four bands Fermi surface (FS) model. We investigate the specific multi-band features and show that distinct length scales of the RKKY oscillations appear. For the regular lattice of the local moments, the generalized RKKY interaction is defined in momentum space. We consider its momentum dependence in paramagnetic and spin density wave (SDW) phases, discuss its implications for the possible type of magnetic order and compare it to the results obtained from more realistic tight-binding type Fermi surface model. Our finding can give important clues on the magnetic ordering of the 4f- iron based superconductors.

PACS numbers: 74.70.Xa, 75.30.Hx,75.30.Fv

1. Introduction

The discovery of iron-based superconductors [1], has lead to a renewed interest in multiband superconductivity [2, 3]. Their parent compounds are paramagnetic metals at high temperature and mostly show an antiferromagnetic (AF) order of spin density wave (SDW) type slightly below a tetragonal to orthorhombic structural transition [4]. Magnetic order of the itinerant Fe moments is driven by the nesting properties of 3d type Fermi surfaces which consist of hole and electron pockets around the center and at the boundaries of the Brillouin zone (BZ). The magnetism of the parent compounds becomes even more involved in rare earth (R) based Fe-pnictides where layers with localized 4f moments exist that are separated from the Fe-As layers with itinerant 3d moments. It is found that the R- moments order at temperatures much below the SDW transition. Their magnetic structure may be generally different from that of the Fe layers. The latter predominantely show the collinear in-plane stripe structure of Fe moments while the R layers may order in different noncollinear or simple ferromagnetic structure. For example the in-plane FM order appears in the 122 family RFe_2As_2 for R = Eu[5], and in the 1111 family RFeAsO the R = Ce compound shows non-collinear in-plane stripe structure[6, 7].

Because of the close connection of magnetic and electronic properties in these kind of materials, investigation of magnetic order and effective coupling mechanism of local moments is a question of great interest. The latter may belong to a periodic sublattice of 4f-elements [8, 9, 7, 5]; doped disordered impurity magnetic moments (diluted magnetic moments) [10, 11, 12], or possibly partially localized 3d electrons on the Fe sublattice originating from an orbitally selective Mott-Hubbard localization.

A well studied example of the 4f- based 122 Fe pnictides is $EuFe_2As_2$, with its highest SDW transition temperature reported at $T_{SDW} = 190$K [5, 13, 14, 15, 16, 17]. The AF ordering of localized 4f- moments (Eu^{2+} with $S = 7/2$) happens at lower temperature, $T_N \approx 20$K, for a *different* wave vector $\mathbf{Q} = (0, 0, 1)$. This means the Eu^{2+}-moments are FM ordered in *ab*-planes which is in contrast to the columnar AF order of Fe itinerant moments [5]. In addition, the relaxational behavior of Eu^{2+} spins in ESR shows a distinct magnetic anisotropy below T_{SDW} [18]. The magnetization anisotropy of Eu spins has a temperature dependency which is changing across the SDW transition temperature [19]. These observations indicate that the SDW transition in the Fe-3d itinerant subsystem may have important effects on the effective coupling of local 4f moments. Evidence for the coupling of the $4f^7$-electron and conduction electrons is also obtained by ESR in the Gd-based 1111 compounds $La_xGd_{1-x}FeAsO$ (Gd^{3+} with spin S = 7/2) [12]. Below $T \sim 6$K, neutron scattering measurements also found the Fe-Nd interaction in NdFeAsO single crystals which force the Nd- moments to be ordered AF with the same *ab*-plane configuration as Fe moments[20].

Since the 4f moments are localized, their direct exchange can be neglected. However one has to consider the indirect Ruderman-Kittel-Kasuya-Yosida (RKKY) interaction [21, 22, 23] of 4f moments via spin polarization of 3d conduction electrons. The

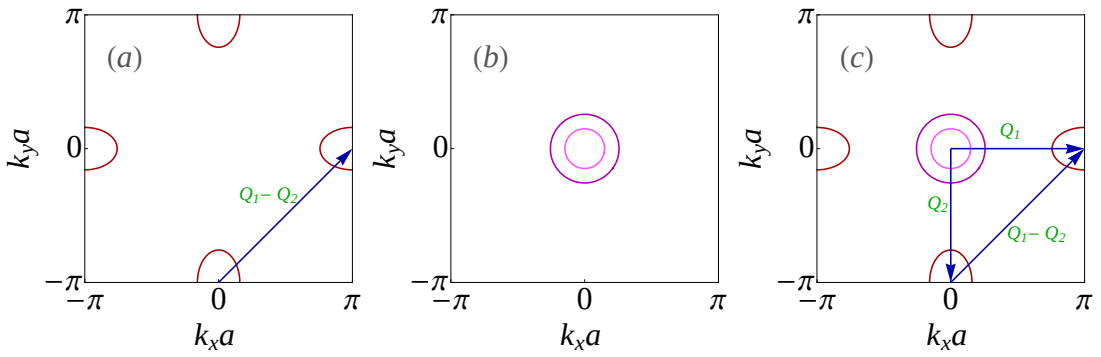

Figure 1. (Color online) a) The Fermi surface with pure electron- like pockets with ellipticity $\epsilon = 0.4$, centered around the $\mathbf{Q}_\beta$ [$\mathbf{Q}_1 = (\pm\pi, 0)$ and $\mathbf{Q}_2 = (0, \pm\pi)$] points in the unfolded BZ (β-bands). b) Fermi surface with pure hole- like pockets centered at Γ- point (α-bands). c) Fermi surface with two circular hole pockets and two electron-like pockets. Note that c) results from a combination of electron and hole pockets in a) and b).

strength of this oscillatory effective exchange is controlled by the distance between two localized 4f moments and the Fermi surface (FS) properties of 3d conduction electrons. Such an interaction generally plays an important role in revealing the nature of the magnetism in metals with partially filled d- and f-electron shells. It is well-known that the RKKY interaction for an anisotropic Fermi surface (FS) with nesting consists of several terms originating from flat regions in the conduction bands (van Hove regions) and those which describe the interference between contributions from their vicinities [24]. For the nearly nested conduction bands the latter term is present down to the interatomic distances and favors the commensurate antiferromagnetic ordering of the localized moments. The degree of nesting varies continuously for different compounds [25], where we have a perfect nesting in some pnictides [26] and weakly nested compound of some chalcogenides[27, 28].

This motivates us to investigate how the RKKY mechanism in iron based superconductors depends on the absence or presence of electron- or hole- Fermi surface sheets and their nesting properties. In most of the iron based superconducting systems, the Fermi surface consists of the hole and electron pockets simultaneously [29, 30, 31, 32, 33, 34, 26]. It is also possible to have a situation with only the hole- like or the electron- like pockets separately. For example, according to band structure calculations [35] and angle resolved photoemission spectroscopy (ARPES) [36] the overdoped KFe_2As_2 compound has no electron - like FS sheets [37]. On the other hand ARPES studies on the alkali-intercalated Fe chalcogenide system KFe_2Se_2 have recently shown that there are no hole- like FS sheets for some doping range [38]. We will use a simplified parabolic band model with isotropic hole but anisotropic electron mass and study how the real space oscillations of RKKY local moment pair interaction evolve with such FS change. We study the general case involving four bands that consist of two

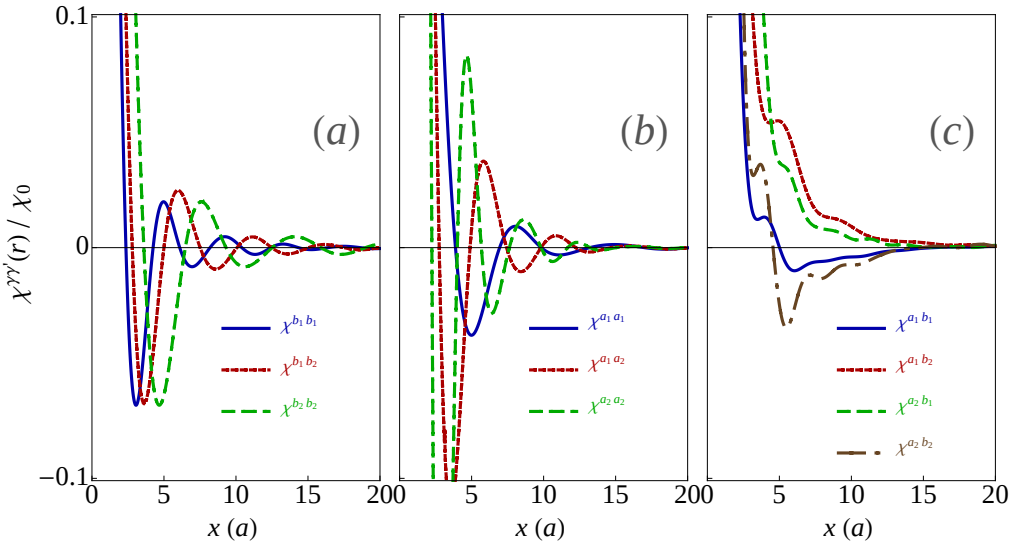

Figure 2. (Color online) The fully analytical calculations of the individual components of magnetic spin susceptibility of conduction electrons $\chi^{\gamma\gamma'}(\mathbf{r})$ (obtained using Eqs.(12, 13) along the x-direction for a) pure electron- like pockets, b) pure hole- like pockets. They are completely in agreement with the numerical results. c) The numerical calculation of the individual components of magnetic spin susceptibility of conduction electrons $\chi^{\gamma\gamma'}(\mathbf{r})$ along the x-direction for only the inter hole- and electron- like contributions. Note that $\chi^{\gamma\gamma'}(\mathbf{r}) = \chi^{\gamma'\gamma}(\mathbf{r})$, furthermore $\chi_0 \equiv \frac{m_e a^2}{4\hbar^2}$.

electron- like and two hole- like sheets. We compare these results with the special case where only one type of sheet is present and the closed analytical solution is obtained.

For a lattice of local moments with effective RKKY interactions the latter will also be analyzed in momentum space. This is relevant for the R-based pnictides with magnetic order appearing both in the itinerant 3d and localized 4f subsystems. These results will be compared to a more detailed calculation using tight-binding type conduction electron bands. As indicated by the above examples the SDW transition and associated gap opening may influence the **q**- dependence and anisotropy of the effective RKKY exchange interaction which determines the type of order in the local moment subsystem. This feedback effect on local moment magnetism will also be investigated for the tight binding model.

2. Model definition

The Hamiltonian describing localized magnetic moments in the multi-band conduction electron sea is given by

$$\mathcal{H} = \mathcal{H}_c + \mathcal{H}_{int}, \tag{1}$$

where $\mathcal{H}_c$ is the conduction electron Hamiltonian according to

$$\mathcal{H}_c = \sum_{\mathbf{k},\gamma,\sigma} \varepsilon^{\gamma}_{\mathbf{k}} c^{\dagger}_{\gamma\mathbf{k}\sigma} c_{\gamma\mathbf{k}\sigma}. \tag{2}$$

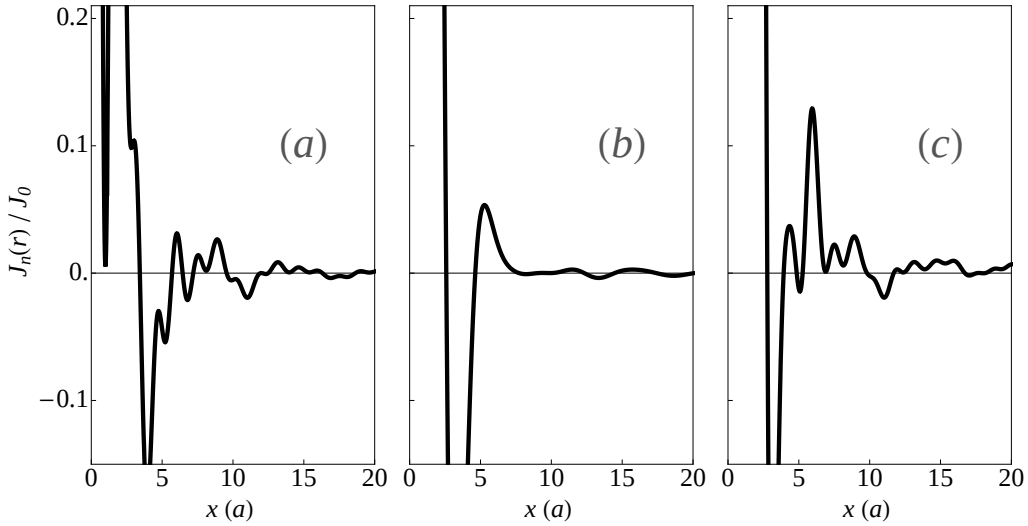

Figure 3. The normalized total RKKY interaction, $J_n(\mathbf{r})/J_0$, for a) pure electron- like pockets, b) pure hole- like pockets and c) for the case with 4 electron and hole bands, corresponding to the case of Fig.(1.c), along the x-direction, furthermore $J_0 \equiv J_{ex}^2\chi_0$. (a) and (c) exhibit rapid oscillations due to the inter-pocket contributions (c. f. Fig. 1a,c)

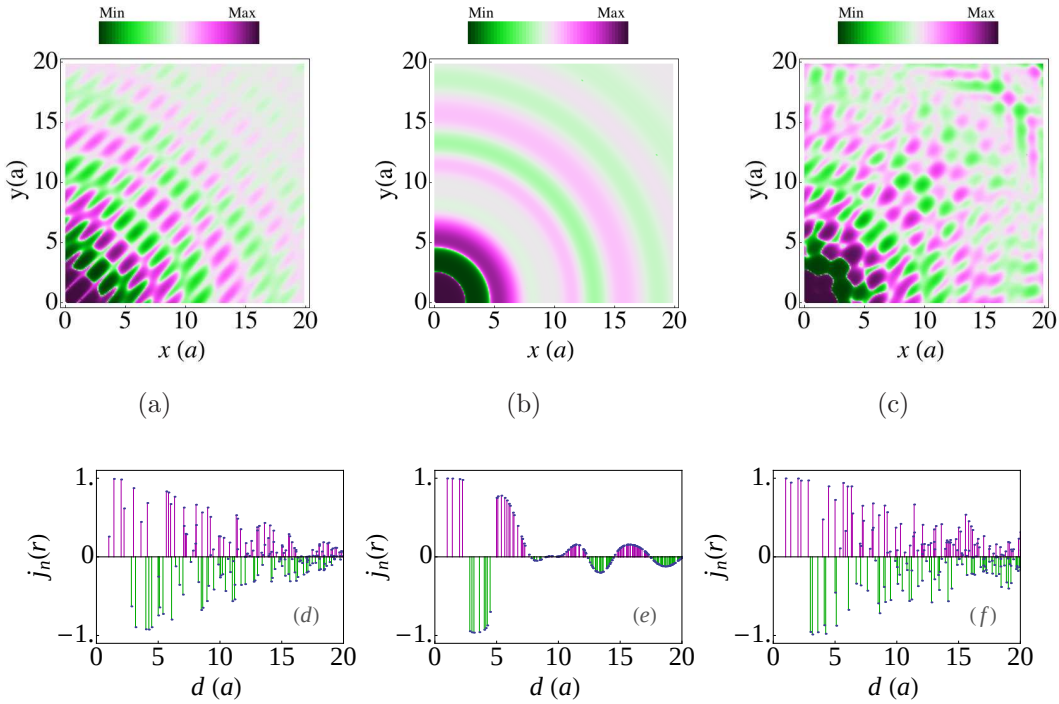

Figure 4. (Color online) The spatial plot of the normalized total RKKY interaction, $j_n(\mathbf{r}) = \frac{J_n(\mathbf{r})}{|J_n(\mathbf{r})|+0.015}$, for a) pure electron- like pockets, b) pure hole- like pockets and c) for the case with 4 electron and hole bands, corresponding to Fig.(1). Bar plots: (d), (e) and (f) present of normalized total RKKY interaction, $\langle j_n(\mathbf{r})\rangle$, for two local moment sitting on the origin and the lattice site $(x, y) = (na, ma); n, m = 0, \pm 1..$ with distance $d = \sqrt{x^2 + y^2}$ corresponding to the plots (a), (b) and (c), respectively.

Here, $c^{\dagger}_{\gamma\mathbf{k}\sigma}$ denotes the creation operators and $\varepsilon^{\gamma}_{\mathbf{k}}$ is the dispersion of conduction electrons with momentum $\mathbf{k} = (k_x, k_y)$ and spin σ in band γ.

In the present work we consider primarily the minimal four-bands model consisting two hole- like pockets centered at Γ- point (α-bands), and two elliptical electron FS pockets centered around $\mathbf{Q}_\beta$ [$\mathbf{Q}_1 = (\pm\pi, 0)$ and $\mathbf{Q}_2 = (0, \pm\pi)$] points in the unfolded Brillouin zone (BZ) (β-bands). We consider three different cases: a) only electron- like FS sheets, b) only hole- like FS sheets, and finally c) both hole and electron FS sheets (see Fig.1). Thus one can rewrite the total conduction electron Hamiltonian Eq.(2) as

$$\mathcal{H}_c = \sum_{\alpha,\mathbf{k},\sigma} \varepsilon^{\alpha}_{\mathbf{k}} a^{\dagger}_{\alpha\mathbf{k}\sigma} a_{\alpha\mathbf{k}\sigma} + \sum_{\beta,\mathbf{k},\sigma} \varepsilon^{\beta}_{\mathbf{k}} b^{\dagger}_{\beta\mathbf{k}\sigma} b_{\beta\mathbf{k}\sigma}, \tag{3}$$

where $a^{\dagger}_{\gamma\mathbf{k}\sigma}$ ($b^{\dagger}_{\gamma\mathbf{k}\sigma}$) creates electrons with spin σ, momentum $\mathbf{k}$ at hole-(electron-) like band α (β). The dispersion of the electrons pockets can be modeled as $\varepsilon^{\beta}_{\mathbf{k}-\mathbf{Q}_\beta} = \frac{\hbar^2 k_x^2}{m_x^{\beta}} + \frac{\hbar^2 k_y^2}{m_y^{\beta}} - \mu_\beta$, and for the hole- like pockets we have $\varepsilon^{\alpha}_{\mathbf{k}} = -[\frac{\hbar^2 k_x^2}{m_x^{\alpha}} + \frac{\hbar^2 k_y^2}{m_y^{\alpha}}] - \mu_\alpha$, where m_n^{γ} denotes the band mass ($n = x, y$) in k_n direction. Furthermore we define $\mu_\beta = \mu + \varepsilon_0$, and $\mu_\alpha = \mu - \varepsilon_0$ where ε_0 and μ are the energy offset and the chemical potential, respectively. We consider for the hole- like pockets $m_n^{\alpha} = m^{\alpha}$ with $m^{a_2} = 3m^{a_1} = 3m_e$, and for the electron- like pockets $m_x^{b_1} = m_y^{b_2} = (1+\epsilon)m_e$, $m_y^{b_1} = m_x^{b_2} = (1-\epsilon)m_e$ with ellipticity ϵ and electron mass m_e. The corresponding general FS is shown in Fig.(1.c).

The interaction between the spin of conduction electrons, $\mathbf{s}(\mathbf{R})$, and the moment of localized f-electrons, $\mathbf{S}_i$, at site $\mathbf{R}_i$ is given by

$$\mathcal{H}_{int} = J_{ex} \sum_{\mathbf{R};i} I(\mathbf{R} - \mathbf{R}_i)\, \mathbf{s}(\mathbf{R}) \cdot \mathbf{S}_i, \tag{4}$$

where the exchange integral $I(\mathbf{R} - \mathbf{R}_i)$ is established by the overlap of 3d conduction and localized 4f electron wave functions. The real overlap of the conduction electron and localized 4f electron wave-functions and therefore $I(\mathbf{R} - \mathbf{R}_i)$ in general is non-zero in a finite volume around the 4f site $\mathbf{R}_i$. This leads to a damping in the effective intersite coupling energies [39, 40, 41]. For simplicity we use here the common approximation of an on-site exchange interaction which can be approximated as $I(\mathbf{R}-\mathbf{R}_i) = J_{ex}\, \delta(\mathbf{R}-\mathbf{R}_i)$. Here J_{ex} is the on-site exchange coupling constant that can be obtained from a more microscopic Anderson-type model [42] by a Schrieffer-Wolff transformation.

3. Spatial and momentum dependence of effective RKKY interaction

The contact exchange interaction with local moments will polarize the conduction states which then leads to an effective RKKY exchange between moments at different sites. It may be obtained by using the standard second-order perturbation theory with respect to $\mathcal{H}_{int}$. Here we consider first the general form of the RKKY interaction of a pair of local moments and its distance dependence for the various FS topologies. In addition we investigate the momentum dependence of the effective RKKY exchange which determines the magnetic structure in a periodic lattice of local moments.

3.1. Localized magnetic moment pairs and the distance dependence of RKKY interaction

In the paramagnetic or normal state regime the effective exchange Hamiltonian of the RKKY interaction which describes the interaction between two local impurity spins at the positions i and j is derived as [24, 43]

$$\mathcal{H}^{ij}_{RKKY} = -J_n(\mathbf{r})\mathbf{S}_i \cdot \mathbf{S}_j, \tag{5}$$

where $\mathbf{r} = \mathbf{R}_i - \mathbf{R}_j = x\hat{\mathbf{x}} + y\hat{\mathbf{y}}$, and the effective exchange couplings are then given by

$$J_n(\mathbf{r}) = \sum_{\gamma\gamma'} \mathcal{J}^{\gamma\gamma'}_n(\mathbf{r}) = J^2_{ex} Re\left(\sum_{\gamma\gamma'} e^{i(\mathbf{Q}_\gamma - \mathbf{Q}_{\gamma'})\cdot\mathbf{r}} \chi^{\gamma\gamma'}(\mathbf{r})\right), \tag{6}$$

here $\chi^{\gamma\gamma'}(\mathbf{r})$ denotes the intra- ($\gamma = \gamma'$) and inter- ($\gamma \neq \gamma'$) magnetic spin susceptibility of conduction electrons (Lindhard response function) which is defined by

$$\chi^{\gamma\gamma'}(\mathbf{r}) = -k_B T \sum_n G_\gamma(\mathbf{r}, i\omega_n) G_{\gamma'}(\mathbf{r}, i\omega_n). \tag{7}$$

Here $\omega_n = \pi T(2n+1)$ is the fermionic Matsubara frequency and

$$G_\gamma(\mathbf{k}, i\omega_n) = \frac{1}{i\omega_n - \varepsilon^\gamma_{\mathbf{k}}}, \tag{8}$$

is the conduction electrons Greens function in momentum representation. After some algebra [44] the real space Greens function can be obtained as

$$G_\gamma(\mathbf{r}, i\omega_n) = \frac{\sqrt{m^\gamma_x m^\gamma_y}}{\pi\hbar^2} K_0(\sqrt{2Z_\gamma(\omega_n)\rho_\gamma}), \tag{9}$$

where $K_0(\ldots)$ is the modified Bessel (Macdonald) function. Here we define $Z_\gamma = \mu_\gamma + i\omega_n$ and $\rho_\gamma = (m^\gamma_x x^2 + m^\gamma_y y^2)/\hbar^2$. In the low temperature regime

$$k_B T \sum_n (\ldots) \longrightarrow \frac{1}{2\pi i}\int_{-i\infty}^{i\infty} d\omega(\ldots),$$

therefore the magnetic spin susceptibility, Eq.(7), can be calculated using the Green's function as [45]

$$\chi^{\gamma\gamma'}(\mathbf{r}) = \frac{1}{2\pi i}\int_{-i\infty}^{i\infty} d\omega G_\gamma(\mathbf{r}, i\omega) G_{\gamma'}(\mathbf{r}, i\omega). \tag{10}$$

The closed analytic expression for the above integral may be obtained in the case of having the same kind of bands, where $\mu_\gamma = \mu_{\gamma'}$ (Fig.1.a or Fig.1.b). Explicitly, using the properties of the modified Bessel functions in the limit of $Z_\gamma \to \mu_\gamma + i0^\pm$, we have

$$K_n(\sqrt{2Z_e\rho_\gamma}) = \frac{\pm\pi i}{2} e^{\pm n\pi i/2} H^{(\pm)}_n(\sqrt{2\mu_\gamma\rho_\gamma}), \tag{11}$$

where $H^{(\pm)}_n(x) = \mathrm{J}_n(x) \pm i\mathrm{Y}_n(x)$ are Hankel functions [46].

In the special case $\rho_\gamma = \rho_{\gamma'}$, by using Eqs. (9,10), the magnetic susceptibility can be written as

$$\chi^{\gamma\gamma'}(\mathbf{r}) = \Phi_{\gamma\gamma'}\Big[\mathrm{J}_0(X_\gamma)\mathrm{Y}_0(X_\gamma) + \mathrm{J}_1(X_\gamma)\mathrm{Y}_1(X_\gamma)\Big], \tag{12}$$

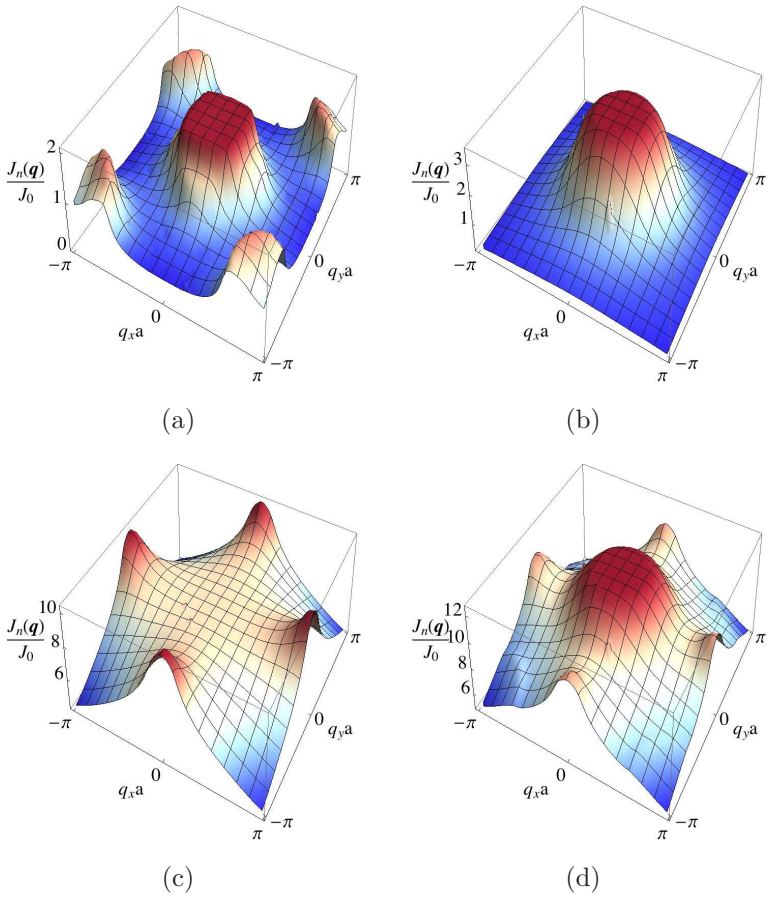

Figure 5. (Color online) The momentum dependency of the Fourier transformation of the total RKKY interaction, $J_n(\mathbf{q})$ for a) pure electron- like pockets, b) pure hole-like pockets c) only the inter hole- and electron- like contributions and d) the to total interaction corresponding to sum of all FS sheet contributions. Results are obtained for the simple parabolic dispersion corresponding to Fig.(1). Absolute maximum of $J_n(\mathbf{q})$ in this simplified model occurs at $\mathbf{q} = 0$ and side maxima at $\mathbf{q} = \mathbf{Q}_\alpha$.

here $\Phi_{\gamma\gamma'} = -\sqrt{m_x^\gamma m_y^\gamma m_x^{\gamma'} m_y^{\gamma'}}\,\frac{\mu_\gamma}{4\pi\hbar^4}$ and $X_\gamma = \sqrt{|2\mu_\gamma\rho_\gamma|}$.

In the general case $\rho_\gamma \neq \rho_{\gamma'}$ we still can find the closed solution

$$\chi^{\gamma\gamma'}(\mathbf{r}) = \frac{\Phi_{\gamma\gamma'}}{X_\gamma^2 - X_{\gamma'}^2} \times \Big[X_\gamma \Big(\mathrm{J}_1(X_\gamma)\mathrm{Y}_0(X_{\gamma'}) + \mathrm{Y}_1(X_\gamma)\mathrm{J}_0(X_{\gamma'}) \Big) - X_{\gamma'} \Big(\mathrm{J}_1(X_{\gamma'})\mathrm{Y}_0(X_\gamma) + \mathrm{Y}_1(X_{\gamma'})\mathrm{J}_0(X_\gamma) \Big) \Big]. \tag{13}$$

For the simple case of spherical FS sheets, i.e. $m_x^\gamma = m_y^\gamma$ we have $X_\gamma = k_f^\gamma r$, where k_f^γ is the Fermi momentum, and $r = \sqrt{x^2 + y^2}$ the distance between local moments.

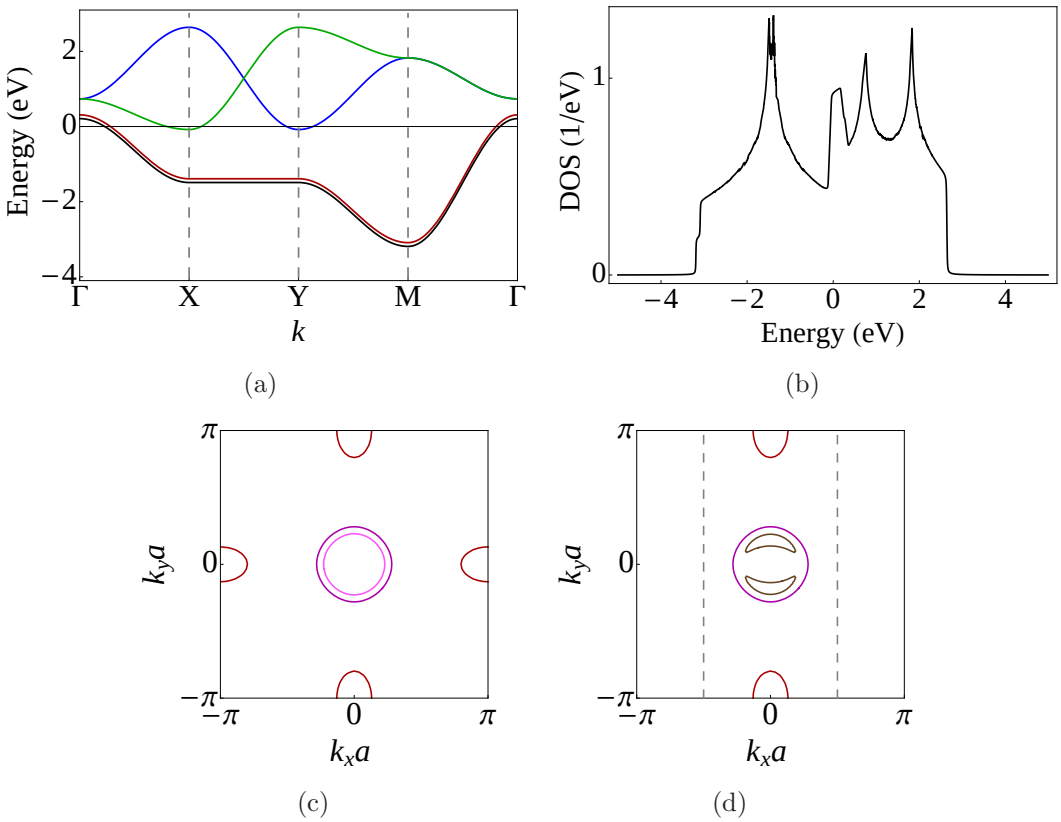

Figure 6. (Color online) (a) A typical tight binding band structure for iron based 122-type superconductors with two circular hole pockets and two electron- like pockets. The BZ symmetry points are $\Gamma(0,0)$, $X(0,\frac{\pi}{a})$, $Y(\frac{\pi}{a},0)$ and $M(\frac{\pi}{a},\frac{\pi}{a})$. The band structure parametrization can be found in Ref.[47]. (b) The corresponding density of states (DOS), and (c) its Fermi surface. (d) The reconstructed FS in the SDW phase with ordering parameter $W = 0.15eV$.

3.2. Periodic lattice of local moments and the momentum dependence of RKKY interaction

In the case of local moments forming a regular lattice it is necessary to go to the momentum representation of the RKKY interaction which is defined by

$$\mathcal{H}_{ff} = -\sum_{ij} J_n(\mathbf{r})\mathbf{S}_i \cdot \mathbf{S}_j = -\sum_{\mathbf{q}} J_n(\mathbf{q})\mathbf{S}_{-\mathbf{q}} \cdot \mathbf{S}_{\mathbf{q}}, \tag{14}$$

where the real space RKKY interaction is given by

$$J_n(\mathbf{r}) = J_{ex}^2 \sum_{\gamma\gamma'} e^{i(\mathbf{Q}_\gamma - \mathbf{Q}_{\gamma'})\cdot\mathbf{r}} \chi^{\gamma\gamma'}(\mathbf{r}), \tag{15}$$

and

$$J_n(\mathbf{q}) = J_{ex}^2 \sum_{\gamma\gamma'} \chi^{\gamma\gamma'}(\mathbf{q} - (\mathbf{Q}_\gamma - \mathbf{Q}_{\gamma'})), \tag{16}$$

is its Fourier transform and $\mathbf{S}_\mathbf{q}$ are the Fourier components of $\mathbf{S}_i$. They are defined by

$$J_n(\mathbf{q}) = \frac{1}{\sqrt{N}} \sum_{\mathbf{r}} J_n(\mathbf{r}) e^{i\mathbf{q}\cdot\mathbf{r}}, \quad S_\mathbf{q} = \frac{1}{\sqrt{N}} \sum_i S_i e^{i\mathbf{q}\cdot\mathbf{R}_i}, \tag{17}$$

respectively, with N denoting the lattice size. The RKKY interaction is proportional to the static conduction electron magnetic susceptibility given by

$$\chi^{\gamma\gamma'}(\mathbf{q}) = -\frac{1}{N}\sum_{\mathbf{k}} \frac{f(\varepsilon^{\gamma}_{\mathbf{k}-\mathbf{q}}) - f(\varepsilon^{\gamma'}_{\mathbf{k}})}{\varepsilon^{\gamma}_{\mathbf{k}-\mathbf{q}} - \varepsilon^{\gamma'}_{\mathbf{k}}}, \tag{18}$$

where $f(\ldots)$ denotes the Fermi function. Here we implied that the electron pocket has been shifted to the Γ- center of the BZ. We may also conveniently define a total susceptibility

$$\chi_t(\mathbf{q}) = \sum_{\gamma\gamma'} \chi^{\gamma\gamma'}(\mathbf{q} - (\mathbf{Q}_{\gamma} - \mathbf{Q}_{\gamma'})). \tag{19}$$

The meaning of $\chi_t(\mathbf{q})$ is twofold: At the wave vector $\mathbf{q}$ where $\chi_t(\mathbf{q})$ acquires its maximum an SDW instability may occur due to 3d conduction electron interactions, opening a SDW gap at FS patches connected by this momentum. Furthermore at the same wave vector the ordering of 4f local moments due to $J_n(\mathbf{q}) = J^2_{ex}\chi_t(\mathbf{q})$ in the rare earth - based Fe pnictides should be expected at lower temperature. Note, however, that due to the feedback effect the opening of the SDW gap may influence the wave vector where $J_n(\mathbf{q})$ has its maximum.

3.3. Momentum dependence of RKKY interaction in spin density wave phase

Recently it was shown [43] that the change of the FS nesting (resulting of the opening of the SDW gap) influences both strength and oscillatory behavior of RKKY in the antiferromagnetic state. In the mean-field approximation the SDW ordering can be described by [48]

$$\mathcal{H}^{MF}_{SDW} = \sum_{\mathbf{k}\sigma} W\sigma \left[a^{\dagger}_{1\mathbf{k}\sigma} b_{1\mathbf{k}+\mathbf{Q}_1\sigma} + H.c.\right], \tag{20}$$

where W is the ordering amplitude and the spin index $\sigma = \pm$ corresponds to spin $\uparrow$ and $\downarrow$. The SDW ordering induces an anisotropy in the RKKY interaction and maps the RKKY into an effective anisotropic XXZ-type Heisenberg exchange model,

$$\begin{aligned}\mathcal{H}_{ff} =& -\sum_{ij}\left[J_x(\mathbf{r})\left(\mathbf{S}^x_i\mathbf{S}^x_j + \mathbf{S}^y_i\mathbf{S}^y_j\right) + J_z(\mathbf{r})\mathbf{S}^z_i\mathbf{S}^z_j\right] \\ =& -\sum_{q}\left[J_x(\mathbf{q})\left(\mathbf{S}^x_{\mathbf{q}}\mathbf{S}^x_{-\mathbf{q}} + \mathbf{S}^y_{\mathbf{q}}\mathbf{S}^y_{-\mathbf{q}}\right) + J_z(\mathbf{q})\mathbf{S}^z_{\mathbf{q}}\mathbf{S}^z_{-\mathbf{q}}\right],\end{aligned} \tag{21}$$

where the momentum dependence of the Fourier transform of the total RKKY interaction in SDW phase is obtained as

$$J_{x,z}(\mathbf{q}) = J^2_{ex}\sum_{\gamma\gamma',\mathbf{k}} \Psi^{x,z}_{\gamma\gamma'\mathbf{k}\mathbf{q}} \frac{f(E^{\gamma}_{\mathbf{k}-\mathbf{q}}) - f(E^{\gamma'}_{\mathbf{k}})}{E^{\gamma}_{\mathbf{k}-\mathbf{q}} - E^{\gamma'}_{\mathbf{k}}}, \tag{22}$$

with the quasiparticle energies defined by $E^3_{\mathbf{k}} = \varepsilon^{b_2}_{\mathbf{k}}$, $E^4_{\mathbf{k}} = \varepsilon^{a_2}_{\mathbf{k}}$, and

$$E^{1,2}_{\mathbf{k}} = \frac{1}{2}\left[(\varepsilon^{a_1}_{\mathbf{k}} + \varepsilon^{b_1}_{\mathbf{k}}) \pm \sqrt{(\varepsilon^{a_1}_{\mathbf{k}} - \varepsilon^{b_1}_{\mathbf{k}})^2 + 4W^2}\right].$$

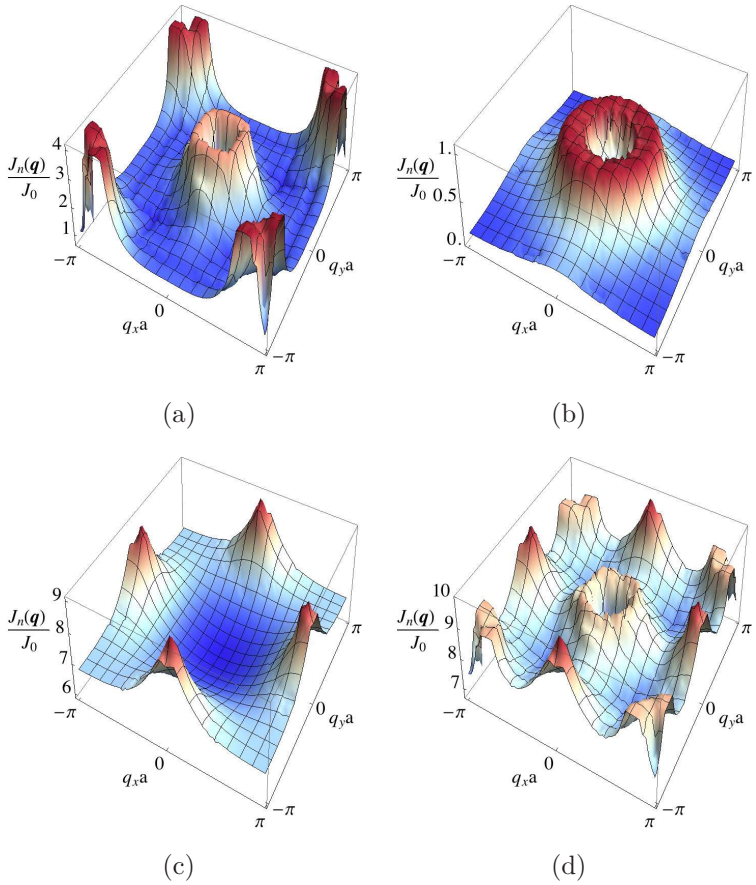

Figure 7. (Color online) The momentum dependence of the Fourier transform of the total RKKY interaction, $J_n(\mathbf{q})$, for a) pure electron- like pockets, b) pure hole-like pockets, c) only the inter hole- and electron- like contributions and d) the total interaction corresponding to sum of all contributions. Results correspond to a typical tight-binding type band structure example (see Fig.(6)) for 122 compounds.

The coherence factors $\Psi^{x,z}_{\gamma\gamma'\mathbf{kq}}$ are given by

$$\Psi^{x}_{\gamma\gamma',\mathbf{k},\mathbf{q}} = \Upsilon^{\gamma}_{\mathbf{k}-\mathbf{q},+}\Upsilon^{\gamma'}_{\mathbf{k},-} + \Upsilon^{\gamma}_{\mathbf{k}-\mathbf{q},-}\Upsilon^{\gamma'}_{\mathbf{k},+}, \tag{23}$$

and

$$\Psi^{z}_{\gamma\gamma',\mathbf{k},\mathbf{q}} = \Upsilon^{\gamma}_{\mathbf{k}-\mathbf{q},+}\Upsilon^{\gamma'}_{\mathbf{k},+} + \Upsilon^{\gamma}_{\mathbf{k}-\mathbf{q},-}\Upsilon^{\gamma'}_{\mathbf{k},-}, \tag{24}$$

with $\Upsilon^{1,2}_{\mathbf{k},\sigma} = (u_{\mathbf{k}} \pm \sigma v_{\mathbf{k}})^2$ and $\Upsilon^{3}_{\mathbf{k},\sigma} = \Upsilon^{4}_{\mathbf{k},\sigma} = 1$. Furthermore the coefficients of the unitary transformation are given by

$$u^2_{\mathbf{k}}, v^2_{\mathbf{k}} = \frac{1}{2}\left[1 \pm \frac{(\varepsilon^{h}_{\mathbf{k}} - \varepsilon^{e_1}_{\mathbf{k}})}{\sqrt{(\varepsilon^{h}_{\mathbf{k}} - \varepsilon^{e_1}_{\mathbf{k}})^2 + 4W^2}}\right]. \tag{25}$$

4. Discussion of numerical results

Now we begin our numerical discussion of the real space and momentum dependence of the RKKY interaction. For the calculations we use $\mu_\gamma = \hbar^2 k_f^{\gamma 2}/2m_e$ with typical

values of Fermi momentum $k_f^\alpha a = 0.15\pi$ for hole (α) - like pockets, and $k_f^\beta a = 0.2\pi$ with ellipticity $\epsilon = 0.4$ for electron (β)- like pockets (Fig.1.). Here a is the lattice constant.

First we present the results for the individual intra- and inter-band contributions to the total spin susceptibility for the various FS models in Fig.(1), they are shown in Fig.(2) in the same sequence. The distance dependence of individual components of $\chi^{\gamma\gamma'}(\mathbf{r})$, along the x-direction is shown in this figure. We notice that the oscillation pattern is similar for intra-band contributions ($\alpha-\alpha, \beta-\beta$), however their maxima and minima are slightly shifted due to the different FS dimensions visible in Fig.(1). This is particularly the case in the inter-band contributions of Fig.(2.c). We note that the results in Figs.(2.a,b) were obtained from the closed analytical expression in Eq. (13) which are identical to the numerical results. For the general FS case with both pockets present $\chi^{\gamma\gamma'}(\mathbf{r})$ can only be calculated numerically.

The total RKKY exchange is proportional to the sum of all ($\gamma\gamma'$) contributions multiplied with a phase factor determined by the pocket distance, i.e., the nesting vectors $\mathbf{Q}_\gamma - \mathbf{Q}_{\gamma'}$. It is shown in Fig.(3) for the three Fermi surface cases of Fig.(1). Fig.(3.a) represents the RKKY interaction for pure electron- like structure. As a result of the extra inter-band ($\beta-\beta$) phase factors in Eq. (15), it shows a new rapid superposed oscillation on top of the fundamental oscillation determined by the FS sheet diameters which is created by summation of individual parts of Fig.(2.a).

For the second case with only hole- like pockets, the total RKKY coupling shows only the oscillations defined by total summation of individual terms. In contrast to the case of electron pockets the rapid oscillations are absent because both (α_1, α_2) hole pockets are Γ- centered without a shift between them.

Finally we present the calculated RKKY interaction for general four band case along the x-direction in the Fig.(3.c). In similar way than in the pure electron case, it shows the combination of slow overall and additional rapid oscillation. The latter originate from both electron-electron ($\beta-\beta$) and electron-hole ($\alpha-\beta$) contribution but not from the hole-hole ($\alpha-\alpha$) part. The size of the electronic pockets and the corresponding Fermi momentum can be changed by tuning the chemical potential. Since the oscillation is defined by the $X_\gamma(\simeq k_f^\gamma r)$ value, an increase of k_f^γ causes the reduction of the wave length of both oscillation types and vice versa.

For a better understanding of the RKKY oscillatory behaviour, in Fig.(4.a-c) we show the full spatial dependency of the normalized total RKKY interaction, $j_n(\mathbf{r}) = \frac{J_n(\mathbf{r})}{|J_n(\mathbf{r})|+\eta}$ (we use the parameter $\eta = 0.015$ for good extremal contrast). Fig.(4.a) is for pure electron- like pockets, Fig.(4.b) is for pure hole- like pockets and Fig.(4.c) is for the general case with 4 electron and hole bands. For a FS with only hole pockets (Fig.(4.b) only long range (radial) oscillations which are almost isotropic appear. When electron pockets are present (Fig.(4.a,c) there are superposed short range oscillations (also azimuthal) due to the interband processes. However a shell-like overall structure of FM/AF regions for moderate distances is preserved, with a notable phase shift by a

half period along the (1,1) direction.

One of the important issues of the diluted system with random local moments (e.g. magnetic impurities like Mn) sitting on lattice sites is the conditon for their magnetic ordering. For this purpose it is useful to know the FM/AF oscillatory RKKY behaviour. Therefore we present the normalized total RKKY interaction, $j_n(\mathbf{r})$, for two local moments sitting at the origin and the lattice site $(x, y) = (na, ma); n, m = 0, \pm 1...$ with a distance $d = \sqrt{x^2 + y^2}$ in the plots of Fig.(4.d-f), respectively. These plots clearly show the change of the interaction form AF to FM by varying the distance of the local moment impurities which is much more rapid when electron like pockets are present. The average impurity distance can be controlled by the concentration of the magnetic impurities in the sample[11].

An experimental determination of the real space variation of the RKKY interaction is sofar not easily possible. However, its Fourier transform is a more accessible quantity, because the magnetic ordering both in the 3d system and in the effectively RKKY coupled 4f system should occur at wave vectors that are maxima of the total static susceptibility $\chi_t(\mathbf{q}) = J_n(\mathbf{q})/J_{ex}^2$, therefore it is useful to calculate $J_n(\mathbf{q})$. The result for the three different contributions from intra-and inter-band transitions to the susceptibility are shown in Fig.(5.a-c). The intra-band contributions have their maximum at the Γ point where the electron part (a) has an additional side maximum at the $\beta - \beta$ nesting vector $\mathbf{Q} = (\pi, \pi)$ which is due to excitations between different electron pockets. The inter-band contribution (c) on the other hand has maxima at the $\mathbf{Q}_\alpha = (\pi, 0), (0, \pi)$, i.e. $\alpha - \beta$ nesting vectors. However the value at the Γ-point $(0, 0)$ is still considerably enhanced. For the general FS of Fig.(1.c) these contributions have to be summed up according to Eq. (19). The resulting total $\chi_t(\mathbf{q}) = J_n(\mathbf{q})/J_{ex}^2$ is shown in Fig.(5.d). Obviously the absolute maximum is still at the Γ point and strongly peaked side maxima at $\mathbf{Q}_\alpha = (\pi, 0), (0, \pi)$ are present. This raises a question about the validity of the simple parabolic electron-hole model discussed so far since the magnetic instability in the 3d system of Fe pnictides is of the SDW type with an ordering vector $\mathbf{Q}_\alpha = (\pi, 0), (0, \pi)$.

To understand this issue better we also calculated the momentum dependence of $\chi_t(\mathbf{q}) = J_n(\mathbf{q})/J_{ex}^2$ in a more realistic tight binding (TB) type band structure for the 3d bands valid for the 122 compounds. The Fermi velocities and size of the pockets in this model are based on Refs.[30, 31, 32]. The band structure and associated density of states (DOS) are presented in Fig.(6). The detailed parametrization can be found in Ref.[47]. The basic features of momentum dependence is similar to the previous model: The maxima occur at or close to zone center due to intra-band processes and at zone boundary points due to nesting features of electron-electron (a) and electron-hole (c) excitations. An essential difference to the parabolic pocket model in Fig.(5c) is the small value of the electron-hole contribution in Fig.(7c) for small momentum transfer. This difference is due to the deep depression in the tight-binding model DOS for $\omega \approx 0$ whereas the DOS for the 2D parabolic band model is simply constant in that region.

As a consequence the absolute maximum of $\chi_t(\mathbf{q}) = J_n(\mathbf{q})/J_{ex}^2$ in the tight-binding case is located at the $\mathbf{Q}_\alpha = (\pi, 0), (0, \pi)$ positions (Fig.7d). Therefore in the latter case the SDW instability of the itinerant 3d electrons is predicted at the proper wave vector.

However the simplified model results in Fig.(5) are nevertheless useful for the understanding of the RKKY interaction because the latter refer to the ordering of localized 4f electrons which takes place only at temperatures much lower than the SDW transition temperature. In the low temperature region the fully developed SDW gap of 3d band electrons will strongly suppress the peak in $\chi_t(\mathbf{q}) = J_n(\mathbf{q})/J_{ex}^2$ at $\mathbf{Q}_\alpha = (\pi, 0)$ (or $(0, \pi)$) because the 'feedback effect' of the gap opening modifies the quasiparticle energies connected by these electron-hole nesting vectors and in fact destroys or reduces the nesting properties for the quasiparticle bands. Therefore deep in the SDW phase the RKKY function will more resemble the one in Fig. (5.d) with the maximum at the Γ point.

This scenario seems indeed to apply to the 4f- based Fe pnictide compound $EuFe_2As_2$. There the AF ordering of itinerant 3d moments takes place below $T_{\mathrm{SDW}} =$ 190K at $\mathbf{Q}_\alpha = (\pi, 0, 0), (0, \pi, 0)$ wave vectors [5]. It is followed by the AF ordering of localized $Eu^{2+}(S = \frac{7}{2})$ 4f- moments at a much lower temperature $T_N \approx 20$K and at a *different* wave vector $\mathbf{q} = (0, 0, 1)$ which means the Eu^{2+} ab-planes with 4f moments are *ferromagnetically* ordered in contrast to the columnar AF order of Fe itinerant 3d moments. This agrees with the arguments given above that the RKKY interaction within the SDW phase is dominated by the broad peak near the Γ -point as presented in Fig. (5.d). This can be fully understood by the feedback effect on the **q**-dependence of the RKKY interaction in the presence of the SDW ordering (Eq.(22)). The SDW couples electron (centered at $\mathbf{Q}_1$) and hole pockets together which leads to reconstructed quasiparticle bands (Sec.3.3). Their associated FS has new small pockets around the Γ-point shown in Fig.(6.d). This causes the RKKY contributions of the involved pockets and the maximum to move to the zone center. The feedback effect of the SDW not only shifts the RKKY maximum to the zone center but also leads to an effective induced RKKY spin space anisotropy as argued in Ref. [43] and experimentally supported in Refs. [19, 18]. This is also observed in the **q**-dependence of RKKY as presented in Fig.(8.a) and Fig.(8.b) for J_x and J_z respectively.

5. Summary

We have investigated the RKKY interaction mechanism in 3d multiband Fe pnictide compounds which is relevant for effective coupling of localized, e.g., 4f moments. We used a simple parabolic band model which allows to describe pure electron, hole and composite Fermi surface models. In the former cases a closed analytical solution for the effective RKKY function was obtained and it is in full agreement with numerical calulation. In the latter case with both electron and hole sheets only numerical evaluation is possible. The RKKY interaction is determined by the sum of two intra-band (e-e and h-h) and two inter-band (e-e and e-h) contributions. The former lead to

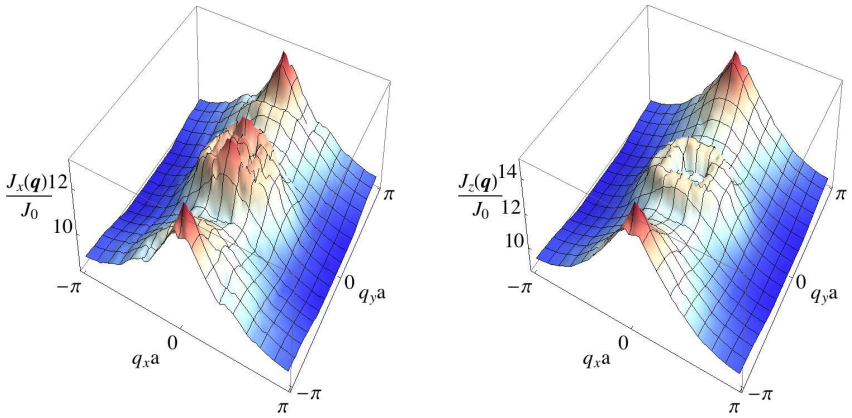

Figure 8. (Color online) The momentum dependence of the Fourier transform of the total RKKY interaction in the SDW phase, correspond to a typical tight-binding type band structure example for 122 compounds, (see Fig.6): a) $J_x(\mathbf{q})$, and b) $J_z(\mathbf{q})$.

slow spatial oscillations determined by the pocket size, the latter to superposed rapid oscillations determined by the inter-pocket nesting vectors. Depending on which Fermi surface sheets are present only the former or both type of oscillations are present in the total RKKY interaction (Fig. 3).

We also studied the momentum dependence of the RKKY interaction which would determine the magnetic order in 4f-based Fe pnictides in a purely 2D picture. We found that in the parabolic band model the maximum of the interaction is at the zone center leading to ferromagnetic order of rare earth planes in these compounds in agreement with observation. A more closer investigation shows that the RKKY interaction derived from a more realistic tight-binding band model would predict a columnar AF order in the plane as for the itinerant Fe moments. However, the feedback mechanism of Fe SDW gap opening on the RKKY interaction shifts the ordering vector to the zone center as obtained in the simplified band model.

It is worthwile to discuss to what extent this purely 2D model analysis may be relevant for the ordering in the 4f based iron pnictides like RFe_2As_2 and RFeAsO. In particular in $EuFe_2As_2$ [5] and CeFeAsO the 4f magnetic order has been investigated. The former is most directly related to the present model because this 122 structure has concerning the local moment properties planar Eu layers. Furthermore the Eu^{2+} state has a pure spin $S = 7/2$ without complications due to crystalline electric field effects and therefore should closely correspond to the effective spin exchange model. In fact this compound exhibits the usual columnar AF SDW order for Fe moments while a much lower T_N=20 K the Eu- moments in each tetragonal ab plane order *ferromagnetically* as predicted by the present effective exchange model and the feedback effect. The stacking along c which is not described in our context is still antiferromagnetic but may also become ferromagnetic by substitution of As with P [19]. The 1111- structure

corresponds less ideally to our model because the Ce atoms do not reside in planar layers. The structure suggests an increased importance of Fe-Ce interlayer coupling which would tend to enforce the columnar AF structure also on the Ce layers. In fact there are large polarization effects of Ce-moments above the Ce ordering temperature due to this coupling [7]. On the other hand the feedback effect still favors ferromagnetic effective exchange within the Ce layers. The resulting non-collinear Ce-ordering below T_N=4 K seems to be a compromise between these two effects; therefore the moments of ferromagnetic Ce columns along b are not opposite along a as in the Fe layers but only perpendicular. We conclude that at least in these two examples the tendency to ferromagnetic effective in-plane exchange found in our model seems to be relevant for the real ordering of 4f moments.

Acknowledgments

We would like to thank D. S. Inosov for useful and stimulating discussions on this work. We are grateful to the Max Planck Institute for the Physics of Complex Systems (MPI-PKS) for the use of computer facilities. A.A. would like to thank the Abdus Salam International Centre for Theoretical Physics (ICTP) for hospitality. I.E. is supported by the Dresden Platform for Superconductivity and Magnetism.

References

[1] Y. Kamihara, T. Watanabe, M. Hirano, and H. Hosono, 2008 *Journal of the American Chemical Society*, 130(11) 3296–3297.
[2] K. Ishida, Y. Nakai, and H. Hosono, 2009 *Journal of the Physical Society of Japan*, 78(6) 062001.
[3] G. R. Stewart, 2011 *Rev. Mod. Phys.*, 83 1589–1652.
[4] M. D. Lumsden and A. D. Christianson, 2010 *Journal of Physics: Condensed Matter*, 22(20) 203203.
[5] Y. Xiao, Y. Su, M. Meven, R. Mittal, C. M. Kumar, T. Chatterji, S. Price, J. Persson, N. Kumar, S. K. Dhar, A. Thamizhavel, and T. Brueckel, 2009 *Phys. Rev B*, 80 174424.
[6] J. Zhao, Q. Huang, C. de la Cruz, S. Li, J. W. Lynn, Y. Chen, M. A. Green, G. F. Chen, G. Li, Z. Li, J. L. Luo, N. L. Wang, and P. Dai, 2008 *Nat Mater*, 7(12) 953–959.
[7] H. Maeter, H. Luetkens, Y. G. Pashkevich, A. Kwadrin, R. Khasanov, A. Amato, A. A. Gusev, K. V. Lamonova, D. A. Chervinskii, R. Klingeler, C. Hess, G. Behr, B. Büchner, and H.-H. Klauss, 2009 *Phys. Rev. B*, 80 094524.
[8] L. Pourovskii, V. Vildosola, S. Biermann, and A. Georges, 2008 *EPL (Europhysics Letters)*, 84(3) 37006.
[9] A. Jesche, C. Krellner, M. de Souza, M. Lang, and C. Geibel, 2009 *New Journal of Physics*, 11(10) 103050.
[10] D. Kitchen, A. Richardella, J.-M. Tang, M. E. Flatte, and A. Yazdani, 2006 *Nature*, 442(7101) 436–439.
[11] Y. Texier, Y. Laplace, P. Mendels, J. T. Park, G. Friemel, D. L. Sun, D. S. Inosov, C. T. Lin, and J. Bobroff, 2012 *EPL (Europhysics Letters)*, 99(1) 17002.
[12] A. Alfonsov, F. Murányi, N. Leps, R. Klingeler, A. Kondrat, C. Hess, S. Wurmehl, A. Köfiler, G. Behr, V. Kataev, and B. Büchner, 2012 *Journal of Experimental and Theoretical Physics*, 114(4) 662.

[13] H. S. Jeevan, Z. Hossain, D. Kasinathan, H. Rosner, C. Geibel, and P. Gegenwart, 2008 *Phys. Rev. B*, 78 052502.
[14] Z. Ren, Q. Tao, S. Jiang, C. Feng, C. Wang, J. Dai, G. Cao, and Z. Xu, 2009 *Phys. Rev. Lett.*, 102 137002.
[15] S. Jiang, Y. Luo, Z. Ren, Z. Zhu, C. Wang, X. Xu, Q. Tao, G. Cao, and Z. Xu, 2009 *New Journal of Physics*, 11(2) 025007.
[16] H. S. Jeevan, D. Kasinathan, H. Rosner, and P. Gegenwart, 2011 *Phys. Rev. B*, 83 054511.
[17] Y. Tokiwa, S.-H. Hübner, O. Beck, H. S. Jeevan, and P. Gegenwart, 2012 *ArXiv e-prints*.
[18] E. Dengler, J. Deisenhofer, H.-A. Krug von Nidda, S. Khim, J. S. Kim, K. H. Kim, F. Casper, C. Felser, and A. Loidl, 2010 *Phys. Rev. B*, 81 024406.
[19] S. Zapf, D. Wu, L. Bogani, H. S. Jeevan, P. Gegenwart, and M. Dressel, 2011 *Phys. Rev B*, 84 140503(R).
[20] W. Tian, W. Ratcliff, M. G. Kim, J.-Q. Yan, P. A. Kienzle, Q. Huang, B. Jensen, K. W. Dennis, R. W. McCallum, T. A. Lograsso, R. J. McQueeney, A. I. Goldman, J. W. Lynn, and A. Kreyssig, 2010 *Phys. Rev. B*, 82 060514.
[21] M. A. Ruderman and C. Kittel, 1954 *Phys. Rev.*, 96 99–102.
[22] T. Kasuya, 1956 *Progress of Theoretical Physics*, 16(1) 45–57.
[23] K. Yosida, 1957 *Phys. Rev.*, 106 893–898.
[24] D. N. Aristov and S. V. Maleyev, 1997 *Phys. Rev. B*, 56 8841–8848.
[25] A. N. Yaresko, G.-Q. Liu, V. N. Antonov, and O. K. Andersen, 2009 *Phys. Rev B*, 79 144421.
[26] A. I. Coldea, J. D. Fletcher, A. Carrington, J. G. Analytis, A. F. Bangura, J.-H. Chu, A. S. Erickson, I. R. Fisher, N. E. Hussey, and R. D. McDonald, 2008 *Phys. Rev. Lett.*, 101 216402.
[27] D. J. Singh, 2012 *Science and Technology of Advanced Materials*, 13(5) 054304.
[28] M. Sadovskii, E. Kuchinskii, and I. Nekrasov, 2012 *Journal of Magnetism and Magnetic Materials*, 324(21) 3481 – 3486.
[29] S. Lebègue, 2007 *Phys. Rev. B*, 75 035110.
[30] D. J. Singh and M.-H. Du, 2008 *Phys. Rev. Lett.*, 100 237003.
[31] L. Boeri, O. V. Dolgov, and A. A. Golubov, 2008 *Phys. Rev. Lett.*, 101 026403.
[32] I. I. Mazin, D. J. Singh, M. D. Johannes, and M. H. Du, 2008 *Phys. Rev. Lett.*, 101 057003.
[33] C. Liu, G. D. Samolyuk, Y. Lee, N. Ni, T. Kondo, A. F. Santander-Syro, S. L. Bud'ko, J. L. McChesney, E. Rotenberg, T. Valla, A. V. Fedorov, P. C. Canfield, B. N. Harmon, and A. Kaminski, 2008 *Phys. Rev. Lett.*, 101 177005.
[34] D. V. Evtushinsky, D. S. Inosov, V. B. Zabolotnyy, A. Koitzsch, M. Knupfer, B. Büchner, M. S. Viazovska, G. L. Sun, V. Hinkov, A. V. Boris, C. T. Lin, B. Keimer, A. Varykhalov, A. A. Kordyuk, and S. V. Borisenko, 2009 *Phys. Rev. B*, 79 054517.
[35] G. Xu, H. Zhang, X. Dai, and Z. Fang, 2008 *EPL (Europhysics Letters)*, 84(6) 67015.
[36] T. Sato, K. Nakayama, Y. Sekiba, P. Richard, Y.-M. Xu, S. Souma, T. Takahashi, G. F. Chen, J. L. Luo, N. L. Wang, and H. Ding, 2009 *Phys. Rev. Lett.*, 103 047002.
[37] J. Guo, S. Jin, G. Wang, S. Wang, K. Zhu, T. Zhou, M. He, and X. Chen, 2010 *Phys. Rev. B*, 82 180520.
[38] T. Qian, X.-P. Wang, W.-C. Jin, P. Zhang, P. Richard, G. Xu, X. Dai, Z. Fang, J.-G. Guo, X.-L. Chen, and H. Ding, 2011 *Phys. Rev. Lett.*, 106 187001.
[39] K. Szalowski and T. Balcerzak, 2008 *Phys. Rev. B*, 78 024419.
[40] S. Smirnov, 2009 *Phys. Rev. B*, 79 134403.
[41] S. Smirnov, 2010 *Phys. Rev. B*, 81 214425.
[42] A. Akbari, I. Eremin, and P. Thalmeier, 2010 *Phys. Rev. B*, 81 014524.
[43] A. Akbari, I. Eremin, and P. Thalmeier, 2011 *Phys. Rev. B*, 84 134513.
[44] D. N. Aristov, 1997 *Phys. Rev. B*, 55 8064–8066.
[45] N. F. Schwabe, R. J. Elliott, and N. S. Wingreen, 1996 *Phys. Rev. B*, 54 12953–12968.
[46] M. Abramowitz and I. Stegun, editors, 1984 *Handbook of Mathematical Functions*. Verlag Harri Deutsch, Thun-Frankfurt am Main.

[47] A. Akbari, J. Knolle, I. Eremin, and R. Moessner, 2010 *Phys. Rev. B*, 82 224506.
[48] I. Eremin and A. V. Chubukov, 2010 *Phys. Rev. B*, 81 024511.